Mon. Not. R. Astron. Soc. **369,** L61–L65 (2006) doi:10.1111/j.1745-3933.2006.00175.x

Discovery of magnetic fields in the β Cephei star ξ^1 CMa and in several slowly pulsating B stars⋆

S. Hubrig,[1]† M. Briquet,[2]‡ M. Schöller,[1] P. De Cat,[3] G. Mathys[1] and C. Aerts[2]

[1]*European Southern Observatory, Casilla 19001, Santiago, Chile*
[2]*Instituut voor Sterrenkunde, Katholieke Universiteit Leuven, Celestijnenlaan 200B, B-3001 Leuven, Belgium*
[3]*Koninklijke Sterrenwacht van België, Ringlaan 3, B-1180 Brussel, Belgium*

Accepted 2006 March 31. Received 2006 March 30; in original form 2006 March 6

ABSTRACT

We present the results of a magnetic survey of a sample of eight β Cephei stars and 26 slowly pulsating B (SPBs) stars with the FOcal Reducer low dispersion Spectrograph at the Very Large Telescope. A weak mean longitudinal magnetic field of the order of a few hundred Gauss is detected in the β Cephei star ξ^1 CMa and in 13 SPB stars. The star ξ^1 CMa becomes the third magnetic star among the β Cephei stars. Before our study, the star ζ Cas was the only known magnetic SPB star. All magnetic SPB stars for which we gathered several magnetic field measurements show a field that varies in time. We do not find a relation between the evolution of the magnetic field with stellar age in our small sample. Our observations imply that β Cephei and SPB stars can no longer be considered as classes of non-magnetic pulsators, but the effect of the fields on the oscillation properties remains to be studied.

Key words: Hertzsprung–Russell (HR) diagram – stars: fundamental parameters – stars: individual: ξ^1 CMa – stars: magnetic fields – stars: oscillations.

1 INTRODUCTION

A long-term monitoring project aimed at asteroseismology of a large sample of slowly pulsating B (SPB) stars and β Cephei stars was started by researchers of the Institute of Astronomy of the University of Leuven several years ago. This initiative started after a number of new pulsating B stars had been discovered by the *Hipparcos* mission (e.g. De Cat & Aerts 2002; Briquet et al. 2003). β Cephei stars are short-period (3–8 h) pulsating variables of spectral type O9 to B3 (8–20 $M_\odot$) along the main sequence with low-order pressure (p) and/or gravity (g) modes. SPB stars are situated in the Hertzsprung–Russell (H–R) diagram just below the β Cephei stars. They are less massive (3–9 $M_\odot$) B-type stars which show variability with periods of the order of 1 d due to multiperiodic high-order low-degree g mode oscillations. Thanks to the *Hipparcos* mission the number of known SPB stars increased from 12 to more than 80 (Waelkens et al. 1998).

The study of the pulsation properties of SPB and β Cephei stars requires observations with a long time-base. Indeed, modes with closely spaced periods occur. As was pointed out by De Cat & Aerts (2002), it is difficult to interpret and explore these multiplets in view of the unknown internal rotation law $\Omega(r)$ and given the dense, theoretically predicted frequency spectra (e.g. Aerts et al. 2006). Recently, Hasan, Zahn & Christensen-Dalsgaard (2005) suggested that high-order g modes are a probe of the internal magnetic field. Their calculations show that frequency splittings of the order of 1 per cent may be due to a poloidal field with a strength of the order of 100 kG, buried in the deep interior of the star.

Neiner et al. (2003a) made the first discovery of a magnetic field in an SPB star. It concerned ζ Cas, the dominant pulsation mode of which has a period $P = 1.56$ d. The two other detections of a magnetic field in pulsating B stars have been achieved for β Cephei stars: β Cep (Henrichs et al. 2000) and V2052 Oph (Neiner et al. 2003b). The measured mean longitudinal magnetic fields in all three stars are weak; less than 100 G. These discoveries motivated us to perform a systematic search for magnetic fields in SPB and β Cephei stars, which started in 2003 with the FOcal Reducer low dispersion Spectrograph (FORS 1) at the Very Large Telescope (VLT). Our recent measurements in the hydrogen lines of various types of stars of intermediate mass demonstrated that magnetic fields can be measured with an error bar as small as 20 G (Hubrig et al. 2006a,b), enabling us to diagnose even very weak mean longitudinal fields. While the latest spectropolarimetric data for our program have been released and reduced only in the last few months, preliminary results of the survey were already presented in Hubrig et al. (2005, 2006b). In this paper we present the whole sample and discuss the results of more than 80 magnetic field measurements.

⋆Based on observations obtained at the European Southern Observatory, Paranal, Chile (ESO programmes 072.D-0377(A), 073.D-0464(A), 073.D-0466(A), and 075.D-0295(A)).

†E-mail: shubrig@eso.org
‡Postdoctoral Fellow of the Fund for Scientific Research of Flanders (FWO).

2 THE SAMPLE OF PULSATING STARS AND OBSERVATIONS

Our sample includes eight β Cephei stars and 26 SPB stars selected from De Cat (2002) such as to fit the observational window and have $V \leqslant 8$. Their fundamental parameters are listed in Table 1. Observations in the Geneva photometric system are available for all targets. The mean Geneva magnitudes were used to obtain the effective temperature $\log(T_{\rm eff})$ and the surface gravity $\log(g)$ with the method described in De Cat (2002) (columns 4 and 5 in Table 1). The $\log(T_{\rm eff})$ and $\log(g)$ values of HD 44743, HD 46005 and HD 46328 are inaccurate because an extrapolation outside the calibration grid was needed. Other stellar parameters were derived from a grid of main-sequence models calculated with the Code Liégeois d'Évolution Stellaire (version 18.2, written by R. Scuflaire) described as 'grid 2' in De Cat et al. (2006). The mass M, the radius R, the luminosity $\log(L/{\rm L}_{\odot})$ and the age of the star expressed as a fraction of its total main-sequence life f are presented in columns 6 to 9 in Table 1. For the most massive stars of our sample, HD 44743, HD 46328 and HD 111123, the upper value of 15 $M_{\odot}$ of the grid models is insufficient to fully cover the observed error box in $\log(T_{\rm eff})$ and $\log(g)$. The stars HD 45284 and HD 46005 fall outside the main sequence. The uncertain parameters are given in *italics* in Table 1. In addition, we point out that the physical parameters of multiple systems (indicated as SB1 and SB2 in column 3 in Table 1), also have to be treated with caution.

For most targets, numerous high-resolution spectroscopic time-series were obtained in previous years (Aerts & De Cat 2003; De Cat & Aerts 2002; Aerts et al. 2004a,b). To estimate the projected rotational velocity $v \sin i$ (column 10 in Table 1), an average of all spectra has been used. For slowly rotating β Cephei and SPB stars, we selected several unblended absorption lines: the λ 4560 Å Si III triplet and/or the λ 4130 Å Si II doublet. For rapidly rotating stars, only the λ 4481 Å Mg I line has been used. We applied the method of

Table 1. Fundamental parameters for the objects in our sample. In the first two columns we give the HD number and another identifier. In the following six columns we list spectral type, effective temperature, surface gravity, mass, radius, and luminosity. The final two columns give the fraction of the main sequence lifetime and $v \sin i$. Uncertain parameter values are given in *italics*.

HD	Other Identifier	Spectral Type	$\log(T_{\rm eff})$	$\log(g)$	$M/{\rm M}_{\odot}$	$R/{\rm R}_{\odot}$	$\log(L/{\rm L}_{\odot})$	f	$v \sin i$ [km s^{-1}]
				β Cephei stars					
29248	ν Eri	B2 III	4.363 ± 0.020	3.92 ± 0.20	10.1 ± 2.2	5.9 ± 2.0	3.9 ± 0.3	0.77 ± 0.16	21 ± 12
44743	β CMa	B1 II-III	*4.421 ± 0.020*	*3.79 ± 0.20*	*13.5 ± 1.5*	*7.5 ± 2.7*	*4.4 ± 0.2*	*0.82 ± 0.17*	11 ± 7
46328	ξ^1 CMa	B1 III	*4.433 ± 0.020*	*3.83 ± 0.20*	*13.7 ± 1.3*	*7.1 ± 2.4*	*4.4 ± 0.2*	*0.76 ± 0.18*	20 ± 7
111123	β Cru	B0.5 III, SB1	4.436 ± 0.020	3.73 ± 0.20	*14.1 ± 0.9*	*7.5 ± 1.8*	*4.4 ± 0.1*	*0.81 ± 0.13*	16 ± 9
129929	V836 Cen	B2	4.379 ± 0.020	4.03 ± 0.20	10.0 ± 2.1	5.1 ± 1.8	3.9 ± 0.3	0.58 ± 0.26	8 ± 5
157056	θ Oph	B2 IV, SB1	4.346 ± 0.020	3.91 ± 0.20	9.4 ± 2.1	5.8 ± 2.0	3.9 ± 0.3	0.79 ± 0.16	16 ± 8
160578	κ Sco	B1.5 III, SB2	4.372 ± 0.020	3.70 ± 0.20	11.6 ± 2.4	7.6 ± 2.2	4.2 ± 0.3	0.91 ± 0.09	97 ± 1
163472	V2052 Oph	B2 IV-V	4.351 ± 0.020	3.86 ± 0.20	10.0 ± 2.2	6.4 ± 2.2	4.0 ± 0.3	0.84 ± 0.13	63 ± 2
				Slowly pulsating B stars					
3379	53 Psc	B2.5I V	4.238 ± 0.020	4.16 ± 0.20	5.4 ± 0.9	3.3 ± 1.0	2.9 ± 0.3	0.45 ± 0.33	33 ± 17
24587	33 Eri	B5 V, SB1	4.142 ± 0.020	4.26 ± 0.20	3.7 ± 0.5	2.5 ± 0.6	2.3 ± 0.3	0.36 ± 0.29	28 ± 1
26326	GU Eri	B5 IV	4.183 ± 0.020	4.14 ± 0.20	4.5 ± 0.7	3.1 ± 1.0	2.6 ± 0.3	0.49 ± 0.32	11 ± 6
28114	V1143 Tau	B6 IV	4.164 ± 0.020	4.00 ± 0.20	4.5 ± 0.8	3.6 ± 1.2	2.7 ± 0.3	0.71 ± 0.23	9 ± 5
34798	YZ Lep	B5 IV-V, SB ?	4.193 ± 0.020	4.25 ± 0.20	4.5 ± 0.6	2.8 ± 0.7	2.6 ± 0.3	0.37 ± 0.28	34 ± 2
45284	BD-07 1424	B8, SB2	4.167 ± 0.020	4.40 ± 0.20	*3.9 ± 0.4*	*2.4 ± 0.3*	*2.4 ± 0.2*	*0.19 ± 0.16*	71 ± 6
46005	V727 Mon	B8 V	*4.326 ± 0.020*	*4.43 ± 0.20*	*7.0 ± 0.7*	*3.2 ± 0.3*	*3.3 ± 0.1*	*0.10 ± 0.07*	–
53921	V450 Car	B9 IV, SB2	4.137 ± 0.020	4.23 ± 0.20	3.7 ± 0.5	2.6 ± 0.7	2.3 ± 0.3	0.39 ± 0.30	17 ± 10
74195	o Vel	B3 IV	4.209 ± 0.020	3.91 ± 0.20	5.5 ± 1.0	4.3 ± 1.4	3.1 ± 0.3	0.82 ± 0.18	9 ± 5
74560	HY Vel	B3 IV, SB1	4.210 ± 0.020	4.15 ± 0.20	4.9 ± 0.8	3.1 ± 1.0	2.8 ± 0.3	0.46 ± 0.32	13 ± 7
85953	V335 Vel	B2 III	4.266 ± 0.020	3.91 ± 0.20	6.8 ± 1.4	4.9 ± 1.7	3.4 ± 0.3	0.81 ± 0.18	18 ± 10
92287	V514 Car	B3 IV, SB1	4.216 ± 0.020	4.00 ± 0.20	5.4 ± 1.0	3.9 ± 1.3	3.0 ± 0.3	0.70 ± 0.23	41 ± 16
123515	V869 Cen	B9 IV, SB2	4.079 ± 0.020	4.27 ± 0.20	3.0 ± 0.4	2.2 ± 0.5	2.0 ± 0.3	0.36 ± 0.28	6 ± 3
131058	ζ Cir	B3 V	4.225 ± 0.020	4.03 ± 0.20	5.5 ± 1.0	3.8 ± 1.3	3.0 ± 0.3	0.66 ± 0.25	264 ± 8
138764	IU Lib	B6 IV	4.148 ± 0.020	4.20 ± 0.20	3.9 ± 0.6	2.7 ± 0.8	2.4 ± 0.3	0.42 ± 0.32	9 ± 5
140873	25 Ser	B8 III, SB2	4.144 ± 0.020	4.35 ± 0.20	3.7 ± 0.4	2.4 ± 0.4	2.3 ± 0.2	0.26 ± 0.21	70 ± 2
143309	V350 Nor	B8/B9 Ib/II	4.147 ± 0.020	4.09 ± 0.20	4.0 ± 0.7	3.0 ± 1.0	2.5 ± 0.3	0.58 ± 0.28	–
160124	V994 Sco	B3 IV-V, SB2	4.171 ± 0.020	4.34 ± 0.20	4.0 ± 0.5	2.5 ± 0.5	2.4 ± 0.2	0.27 ± 0.23	8 ± 4
161783	V539 Ara	B2 V, SB2	4.246 ± 0.020	4.09 ± 0.20	5.7 ± 1.1	3.6 ± 1.2	3.0 ± 0.3	0.56 ± 0.29	–
169820	BD+14 3533	B9 V	4.071 ± 0.020	4.26 ± 0.20	2.9 ± 0.4	2.2 ± 0.6	1.9 ± 0.3	0.37 ± 0.29	–
177863	V4198 Sgr	B8 V, SB1	4.127 ± 0.020	4.14 ± 0.20	3.7 ± 0.6	2.8 ± 0.9	2.3 ± 0.3	0.51 ± 0.30	63 ± 2
181558	V4199 Sgr	B5 III	4.167 ± 0.020	4.16 ± 0.20	4.2 ± 0.7	2.9 ± 1.0	2.5 ± 0.3	0.46 ± 0.34	6 ± 4
182255	3 Vul	B6 III, SB1	4.150 ± 0.020	4.23 ± 0.20	3.9 ± 0.6	2.6 ± 0.7	2.4 ± 0.3	0.39 ± 0.31	10 ± 6
206540	BD+10 4604	B5 IV	4.146 ± 0.020	4.11 ± 0.20	4.0 ± 0.7	3.0 ± 1.0	2.5 ± 0.3	0.55 ± 0.29	8 ± 5
208057	16 Peg	B3 V, SB ?	4.222 ± 0.020	4.15 ± 0.20	5.1 ± 0.8	3.2 ± 1.0	2.8 ± 0.3	0.46 ± 0.33	104 ± 6
215573	ξ Oct	B6 IV	4.145 ± 0.020	4.09 ± 0.20	4.0 ± 0.7	3.0 ± 1.0	2.5 ± 0.3	0.58 ± 0.28	5 ± 2

least-squares fitting with rotationally broadened synthetic profiles using a Gaussian intrinsic width but without taking into account pulsational broadening.

The spectropolarimetric observations were carried out from 2003 to 2005 at the European Southern Observatory with FORS 1 mounted on the 8-m Melipal telescope of the VLT. This multimode instrument is equipped with polarization analyzing optics comprising super-achromatic half-wave and quarter-wave phase retarder plates, and a Wollaston prism with a beam divergence of 22 arcsec in standard resolution mode. In 2003 and 2004, we used the GRISM 600B in the wavelength range 3480–5890 Å to cover all hydrogen Balmer lines from Hβ to the Balmer jump. The highest spectral resolution of the FORS 1 spectra achieved with this setting is $R \sim 2000$. As of 2005 April, we used the GRISM 1200g to cover the H Balmer lines from Hβ to H8, and the narrowest available slit width of 0.4 arcsec to obtain a spectral resolving power of $R \sim 4000$. Usually, we took four to eight continuous series of two exposures for each sample star using a standard readout mode with high gain (A,1 × 1,high) and with the retarder waveplate oriented at two different angles, $+45^\circ$ and -45°. For the observations carried out in 2005, we used a non-standard readout mode with low gain (A,1 × 1,low), which provided a broader dynamic range and increased the signal-to-noise (S/N) ratio of individual spectra by a factor of $\approx$2. All sample stars are bright and, because the errors of the measurements of the polarization with FORS 1 are determined by photon counting statistics, a S/N ratio of a few thousand was reached within $\sim$30 min.

Table 2. The mean longitudinal field measurements for our sample of β Cephei and SPB stars observed with FORS 1 (ESO service programs 072.D-0377, 073.D-0464, 073.D-0466, and 075.D-0295). The first two columns list the HD number and the modified Julian date of mid-exposure. The measured mean longitudinal magnetic field $\langle B_1 \rangle$ is presented in column 3. If there are several measurements for a single star, we give the rms longitudinal magnetic field and the reduced χ^2 for all measurements in columns 4 and 5.

HD	MJD	$\langle B_1 \rangle$ [G]	$\overline{\langle B_l \rangle}$ [G]	χ^2/n	HD	MJD	$\langle B_1 \rangle$	$\overline{\langle B_l \rangle}$ [G]	χ^2/n [G]
3379	53244.402	272 ± 57	182	13.5	129929	53454.199	-52 ± 38	67	3.5
	53245.214	231 ± 47				53572.053	-80 ± 35		
	53629.305	5 ± 22			131058	53454.220	-106 ± 46		
	53630.195	-67 ± 25			138764	52904.016	146 ± 57		
24587	52971.071	-120 ± 68	72	1.5	140873	53151.192	286 ± 60	231	13.4
	53574.415	-16 ± 36				53454.247	-158 ± 78		
	53630.250	-32 ± 29			143309	53151.192	-196 ± 90	113	1.7
26326	52909.389	-119 ± 80	72	1.3		53225.056	85 ± 95		
	53218.357	-24 ± 99				53234.019	-75 ± 73		
	53630.370	-27 ± 22				53454.280	-8 ± 35		
28114	53638.390	-58 ± 21			157056	53532.324	-39 ± 21		
29248	53629.322	-41 ± 28	33	1.6	160124	53151.259	456 ± 60	232	15.5
	53630.347	-22 ± 21				53520.230	-77 ± 45		
34798	52999.055	56 ± 82	125	3.6		53600.109	19 ± 36		
	53218.406	-205 ± 98				53604.108	-25 ± 24		
	53638.366	-41 ± 17			160578	53532.342	-45 ± 41	73	3.3
44743	53475.029	24 ± 70	35	1.2		53604.127	93 ± 40		
	53629.343	-44 ± 29			161783	53151.281	376 ± 63	210	14.6
45284	53252.365	245 ± 63				53487.333	-88 ± 31		
46005	53259.399	2 ± 79				53520.308	-113 ± 32		
46328	53475.046	280 ± 44	306	47.1		53598.108	-122 ± 78		
	53506.971	330 ± 45			163472	53151.298	121 ± 54		
53921	52999.137	-294 ± 63	185	25.3	169820	53151.312	239 ± 70	147	5.3
	53475.100	-71 ± 87				53520.333	-86 ± 45		
	53630.401	151 ± 29				53597.112	-26 ± 34		
	53631.408	151 ± 21			177863	53193.211	-21 ± 54	44	2.7
74195	53002.127	-277 ± 108	200	5.0		53597.128	-59 ± 26		
	53138.972	-310 ± 98			181558	53193.251	-114 ± 50	201	8.4
	53143.972	-145 ± 70				53227.184	236 ± 75		
	53454.107	-65 ± 39				53274.144	-247 ± 98		
	53455.080	-44 ± 37				53275.143	-336 ± 63		
74560	53002.141	-199 ± 61	146	5.6		53519.376	0 ± 34		
	53143.986	-53 ± 66				53520.397	-26 ± 31		
85953	53002.152	-131 ± 42	103	6.1	182255	53193.234	-13 ± 57		
	53152.970	-151 ± 49			206540	53514.416	-51 ± 31		
	53454.137	-52 ± 23			208057	53192.307	104 ± 66	133	13.9
	53455.109	10 ± 21				53597.166	-156 ± 31		
92287	53008.352	-10 ± 57	37	2.8	215573	52900.080	165 ± 53	174	6.9
	53454.152	-52 ± 22				53191.222	180 ± 54		
111123	53455.155	-14 ± 38	18	0.2		53192.290	123 ± 66		
	53475.154	22 ± 51				53193.321	-320 ± 90		
123515	52824.093	-59 ± 50	43	0.9		53506.414	60 ± 45		
	53454.179	17 ± 27				53522.420	-36 ± 21		

More details on the observing technique with FORS 1 can be found elsewhere (e.g. Bagnulo et al. 2002; Hubrig et al. 2004). Determination of the longitudinal magnetic field using the FORS 1 spectra is achieved by measuring the circular polarization of opposite sign induced in the wings of hydrogen Balmer lines by the Zeeman effect. The mean longitudinal magnetic field is the average over the stellar hemisphere visible at the time of observation of the component of the field parallel to the line of sight, weighted by the local emergent spectral line intensity. It is diagnosed from the slope of a linear regression of V/I versus the quantity $-g_{\rm eff}\Delta\lambda_z\lambda^2(1/I)\mathrm{d}I/\mathrm{d}\lambda\langle B_l\rangle + V_0/I_0$,where V is the Stokes parameter which measures the circular polarization, I is the intensity observed in unpolarized light, $g_{\rm eff}$ is the effective Landé factor, λ is the wavelength, $\mathrm{d}I/\mathrm{d}\lambda$ is the derivative of Stokes I, and $\langle B_l\rangle$ is the mean longitudinal field. Our experience of studying a large sample of magnetic and non-magnetic Ap and Bp stars revealed that this regression technique is very robust and that detections with $B_l > 3\sigma$ result only for stars possessing magnetic fields.

3 ANALYSIS AND RESULTS

The mean longitudinal magnetic field $\langle B_l\rangle$ of the targets is listed in Table 2. The rms longitudinal field is computed from all n measurements according to

$$\overline{\langle B_l\rangle} = \left(\frac{1}{n}\sum_{i=1}^{n}\langle B_l\rangle_i^2\right)^{1/2}. \quad (1)$$

Further, in column 5 we give the reduced χ^2 for these measurements, which is a statistical discriminant useful to assess the presence of a magnetic field (Bohlender, Landstreet & Thompson 1993), defined as:

$$\chi^2/n = \frac{1}{n}\sum_{i=1}^{n}\left(\frac{\langle B_l\rangle_i}{\sigma_i}\right)^2. \quad (2)$$

A longitudinal magnetic field at a level larger than 3σ has been diagnosed for 13 SPB stars: HD 3379, HD 45284, HD 53921, HD 74195, HD 74560, HD 85953, HD 140873, HD 160124, HD 161783, HD 169820, HD 181558, HD 208057 and HD 215573. The star HD 208057 has a rather high v sin i value and was classified as a Be star by Merrill & Burwell (1943) due to the detection of double emission in Hα. Although the emissison was not confirmed in later observations, it cannot be ruled out that this star is a Be star. Given the still uncertain status of the magnetic field discovered by Neiner et al. (2003c) in ω Ori, HD 208057 is possibly the first Be star with a magnetic field detected at the 3σ level.

Most stars with multiple measurements have $\chi^2/n \geqslant 5.0$. The individual measurements show the variability of their magnetic field. The time-scales of these variations are uncertain due to too few measurements being obtained for each star. Unfortunately, the rotational variability of the magnetic field cannot be proven either, as the rotational periods are not known for any of these targets. For the SPB star HD 181558, which has the largest number of magnetic field measurements (six in all), we searched for a correlation between the changes of the magnetic field with the pulsation period, but no clear correlation could be detected.

The magnetic field of ξ^1 CMa is detected at a greater than 6σ level. Both measurements carried out on two nights separated by about one month are of the order of 300 G. In Fig. 1 we present Stokes I and V spectra and the regression detection. Spectroscopic and photometric observations revealed that ξ^1 CMa pulsates monoperiodically and non-linearly in a radial mode with a period of 0.209574 d, with a velocity amplitude of 33 km s^{-1} (Saesen, Briquet & Aerts 2006). Morel et al. (2006) performed an abundance analysis of nine selected β Cephei stars and discovered ξ^1 CMa to be nitrogen enriched, as well as the three β Cephei stars δ Cet, V2052 Oph and β Cep. It is remarkable that two of them, V2052 Oph and β Cep, also have a detected longitudinal magnetic field of the order of $\sim$100 G (Neiner et al. 2003b; Henrichs et al. 2000). ξ^1 CMa shows the largest mean longitudinal field by a factor of three among these three β Cephei stars. Unfortunately, no search for a magnetic field has been attempted yet for δ Cet. These four stars have another common property: they are either radial pulsators (ξ^1 CMa) or their multiperiodic pulsations are dominated by a radial mode (δ Cet, β Cep and V2052 Oph). The presence of a magnetic field in these stars might play an important role in explaining these physical characteristics.

The position of the studied SPB and β Cephei stars in the H–R diagram is shown in Fig. 2. No clear picture emerges concerning the evolutionary stage of stars with detected magnetic fields. We have to note, however, that the uncertainties of the age of hot stars (Table 1, column 9) are very large. Furthermore, the whole sample under study contains only 14 stars with detected magnetic fields, so there is a need for more magnetic field measurements to have good statistics. No hints of relations between the magnetic field strength and other stellar parameters were found. Despite our discovery, the knowledge of the magnetic fields in pulsating B stars remains very incomplete. Magnetic fields are known to play an important role in the theoretical interpretation of the pulsations in cool, rapidly oscillating Ap stars.

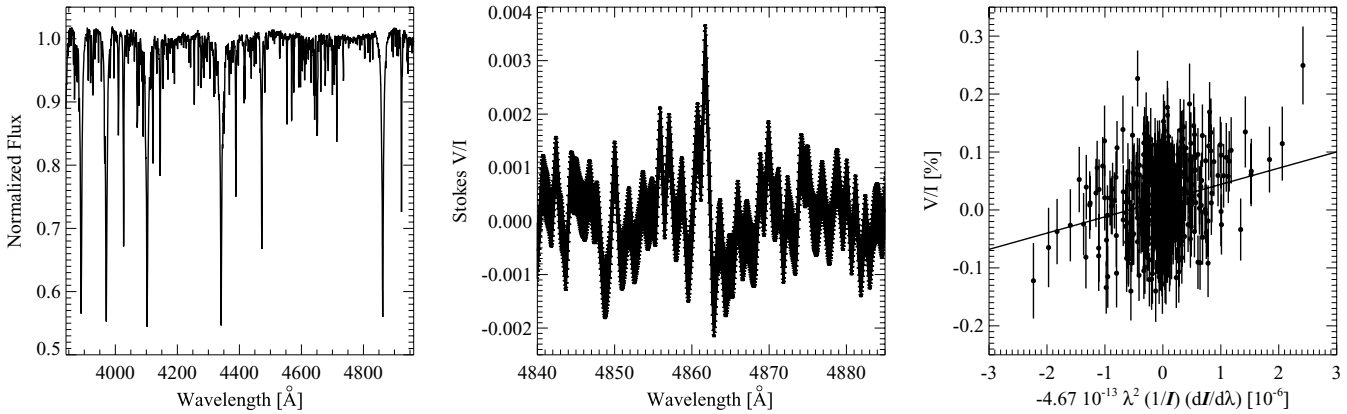

Figure 1. Stokes I spectrum (left), Stokes V spectrum (centre) and regression detection (right) for ξ^1 CMa. The thickness of the plotted line in the Stokes V spectrum corresponds to the uncertainty of the measurement of polarization determined from photon noise.

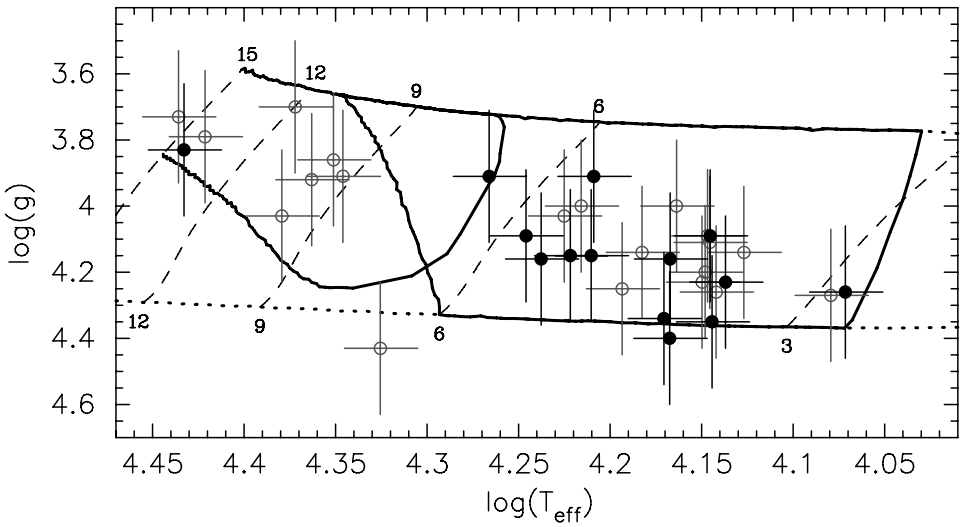

Figure 2. The position of the targets in the H–R diagram. The full lines represent boundaries of theoretical instability strips for modes with frequency between 0.2 and 30 d^{-1} and $\ell \leqslant 3$, computed for main-sequence models with $2\,M_\odot \leqslant M \leqslant 15\,M_\odot$ of 'grid 2' in De Cat et al. (2006). The lower and upper dotted lines show the zero-age main sequence and terminal-age main sequence, respectively. The dashed lines denote evolution tracks for stars with $M = 15$, 12, 9, 6, and $3\,M_\odot$. Filled circles correspond to the stars with detected magnetic fields.

It is difficult to explain why non-pulsating chemically peculiar hot Bp stars and pulsating stars co-exist in the SPB and β Cephei instability strips. It is especially intriguing that the magnetic fields of hot Bp stars either do not show any detectable variations or vary with periods of close to 1 d, which is of the order of the pulsation period range of SPB stars (Bohlender et al. 1987; Matthews & Bohlender 1991). The presented magnetic field measurements in 13 SPB stars and in the β Cephei star ξ^1 CMa demonstrate that longitudinal magnetic fields in these stars are rather weak in comparison to the kG fields detected in magnetic Bp stars.

Although the magnetic field determination method based on circularly polarized FORS 1 spectra of hydrogen Balmer lines shows the excellent potential of FORS 1 for the detection of weak fields, it would be particularly important to measure the fields with higher resolution spectropolarimeters, not only using hydrogen lines but also lines of other chemical elements, to be able to study the field configuration at high confidence levels.

The role of the detected magnetic fields in the modelling of the oscillations of B-type stars remains to be studied. The magnetoacoustic coupling in pulsating B stars will be far less important than for the roAp stars. The effect on the p modes of the β Cephei stars is expected to be small (Hasan & Christensen–Dalsgaard 1992) but the g modes of the SPB stars may be slightly affected, provided that the internal field strength is a factor of 1000 larger than the detected value (Hasan et al. 2005). In any case, magnetic breaking and angular momentum transport along the field lines now offer a natural explanation of the slow rotation of our target stars.

REFERENCES

Aerts C., De Cat P., 2003, SSRv, 105, 453
Aerts C. et al., 2004a, MNRAS, 347, 463
Aerts C. et al., 2004b, A&A, 415, 241
Aerts C. et al., 2006, ApJL, in press
Bagnulo S., Szeifert T., Wade G. A., Landstreet J. D., Mathys G., 2002, A&A, 389, 191
Bohlender D. A., Landstreet J. D., Brown D. N., Thompson I. B., 1987, ApJ, 323, 325
Bohlender D. A., Landstreet J. D., Thompson I. B., 1993, A&A, 269, 355
Briquet M., Aerts C., Mathias P., Scuflaire R., Noels A., 2003, A&A, 401, 281
De Cat P., 2002 in Aerts C., Bedding T. R., Christensen-Dalsgaard J., eds, ASP Conf. Ser. Vol. 259, Radial and Nonradial Pulsations as Probes of Stellar Physics. Astron. Soc. Pac., San Francisco, p. 196
De Cat P., Aerts C., 2002, A&A, 393, 965
De Cat P. et al., 2006, Commun. Asteroseismology, 147, 48
Hasan S. S., Christensen-Dalsgaard J., 1992, ApJ, 396, 311
Hasan S. S., Zahn J.-P., Christensen-Dalsgaard J., 2005, A&A, 444, L29
Henrichs H. F. et al., 2000, in Smith M. A., Henrichs H. F., eds, ASP Conf. Ser. Vol. 214, The Be Phenomenon in Early-Type Stars. Astron. Soc. Pac., San Francisco, p. 324
Hubrig S., Szeifert T., Schöller M., Mathys G., Dziembowski W. A., 2004, A&A, 415, 661
Hubrig S., Szeifert T., North P., Schoeller M., Yudin R.V., 2005, in Ignace R., Gayley K. G., eds, ASP Conf. Ser. Vol. 337, The Nature and Evolution of Disks Around Hot Stars. Astron. Soc. Pac., San Francisco, p. 236
Hubrig S., North P., Schöller M., Mathys G., 2006a, AN, 327, 289
Hubrig S., Yudin R.V., Schöller M., Pogodin M. A., 2006b, A&A, 446, 1089
Matthews J. M., Bohlender D. A., 1991, A&A, 243, 148
Merrill P. W., Burwell C. G., 1943, ApJ, 98, 153
Morel T., Butler K., Aerts C., Neiner C., Briquet M., 2006, A&A, submitted
Neiner C., Geers V. C., Henrichs H. F., Floquet M., Frémat Y., Hubert A.-M., Preuss O., Wiersema K., 2003a, A&A, 406, 1019
Neiner C. et al., 2003b, A&A, 411, 565
Neiner C., Hubert A.-M., Frémat Y., Floquet M., Jankov S., Preuss O., Henrichs H. F., Zorec J., 2003c, A&A, 409, 275
Saesen S., Briquet M., Aerts C., 2006, Commun. Asteroseismology, 147, 109
Waelkens C., Aerts C., Kestens E., Grenon M., Eyer L., 1998, A&A, 330, 215

This paper has been typeset from a TEX/LATEX file prepared by the author.